Available online at www.sciencedirect.com
SCIENCE DIRECT®
Spectrochimica Acta Part A 61 (2005) 1207–1217
SPECTROCHIMICA ACTA PART A
www.elsevier.com/locate/saa

Structure and stability of arthropodan hemocyanin *Limulus polyphemus*

Pavlina Dolashka-Angelova [a,*], Alexander Dolashki [b], Stefan Stevanovic [c], Rumijana Hristova [a], Boris Atanasov [a,1], Peter Nikolov [a], Wolfgang Voelter [b]

[a] *Institute of Organic Chemistry, Bulgarian Academy of Sciences, Acad. G. Bonchev, street, bldg. 9, 1113 Sofia, Bulgaria*
[b] *Abteilung für Physikalische Biochemie, Physiologisch-chemisches Institut der Universität Tübingen, Hoppe-Seyler-Straße 4, 72076 Tübingen, Germany*
[c] *Department of Immunology, Institute for Cell Biology, University of Tübingen, Auf der Morgenstelle 15, D-72076 Tübingen, Germany*

Received 17 March 2004; accepted 14 June 2004

Abstract

In the hemolymph of many arthropodan species, respiratory copper proteins of high molecular weight, termed hemocyanins (Hcs) are dissolved. In this communication, we report on the protein stability of different hemocyanin species (Crustacea and Chelicerata) using fluorescence spectroscopy. Five to seven major electrophoretically separable protein chains (structural subunits) were purified by fast protein liquid chromatography (FPLC) ion exchange chromatography from different hemocyanins with very high sequence homology of the active site regions binding copper ions (CuA and CuB), and especially the relative sequence positions of histidine (His) and tryptophan (Trp) residues of these protein segments are in all cases identical. The conformational stabilities of the native dodecameric aggregates and their isolated structural subunits towards various denaturants (pH and guanidine hydrochloride (Gdn.HCl)) indicate that the quaternary structure is stabilized by hydrophilic and polar forces, whereby both, the oxy- and apo-forms of the protein are considered. These two classes of Crustacea and Chelicerata Hcs have the similar Trp-fluorescence quantum yields, but different values of λ_{max} emission (about 325 and 337 nm, respectively). Differences in the quantum yields are observed of the oxy- and apo-forms, which must be attributed to the fluorescence quenching effect of the two copper ions (CuA and CuB) in the active site. The position of emission maximum indicates tryptophan side chains are situated in a non-polar environment. Denaturation studies of Hcs by Gdn.HCl indicate that the denaturation process consists of two steps: dissociation of the native molecule into its structural subunits and denaturation of the subunits at concentrations >1.5 M Gdn.HCl. Two steps of denaturation are also observed after keeping the protein in buffer solutions at different pH values with different pH-stability for holo-oxy and apo-Hc forms.

Keywords: Arthropods; Molluscs; Hemocyanins; Protein stability/denaturation; Trp-fluorescence

1. Introduction

The circulatory transport of oxygen is essential for efficient aerobic metabolism in most animals. Most intensively investigated are the hemoglobins while hemerythrins and hemocyanins (Hcs) are less studied oxygen-carrying protein classes. The hemocyanins are extracellular, copper-containing proteins of high molecular weight that occur in the hemolymph of many arthropodan and molluscan species [1,2]. Arthropodan Hcs are aggregates of hexameric building blocks, referred to as 16S species, according to their sedimentation coefficients. Higher aggregation forms of the 16S

Abbreviations: A, aggregate; AA, amino acid residue(s); N-Ac-Trp.NH_2, N-acetyl tryptophan amide; CuA and CuB, copper ions in the active sites A and B; λ_{ex}, excitation wavelength (in nm); Hc(s), hemocyanin(s); His, histidine; Gdn.HCl, guanidine hydrochloride; τ, lifetime; Mn′, native monomer; Mu, unfolded monomer; $pH_{d,a}$ and $pH_{d,b}$, acid and basic pH of denaturation; Tn, native tetramer; Tn′, intermediate tetramer; Tyr, tyrosine; Trp, tryptophan

* Corresponding author. Tel.: +359 2 9606163; fax: +359 2 8700225.
E-mail addresses: pda54@yahoo.com (P. Dolashka-Angelova), boris@orgchm.bas.bg (B. Atanasov).
[1] Co-corresponding author.

1386-1425/$ – see front matter © 2004 Published by Elsevier B.V.
doi:10.1016/j.saa.2004.06.043

species are the 24S dimers (or 2 × 6-mers), the 37S tetramers (or 4 × 6-mers) and the 62S octamers (or 8 × 6-mers), stabilized by Ca^{2+} ions. A specific aggregation form is typical for each species of the phylum; the higher molecular weight oligomers can be reversibly dissociated into the 16S species under mild conditions by removing Ca^{2+} at neutral pH. The 16S species ($M_r \sim 450$ kDa) are composed of six 5S subunits ($M_r \sim 75$ kDa), each containing one oxygen-binding site and arranged as a trigonal antiprism [2–4]. The 5S subunit consists of a single polypeptide chain of about 660 residues, forming three structural domains by folding. Different kinds of 5S subunits exist in the various Hc species differing from each other by their association/dissociation behaviours, as documented elsewhere [3]. Four subphyla of arthropodan Hcs have been identified. Three classes of them, Crustacea, Chelicerata and Myriapoda have been studied, while little is known from Hexapoda [5]. *Limulus polyphemus* Chelicerata Hc is one of the most complex species, composed of 8 hexamers or 48 structural subunits [6,7]. Studies on the atomic coordinates of the oxy- and deoxy-forms of subunit II of *Limulus* hemocyanin has provided intriguing insights concerning oxygen binding, allosteric control of oxygen affinity and effects that stabilize the oxygen-binding active site [8].

Subunit II of horseshoe crab *L. polyphemus* shows considerable sequence homology with subunit A of Chelicerata Hc *Euyrypelma californicum* (99%) and with subunit A of Crustacea *Panulirus* Hc. Xiphosura (*L. polyphemus*) and Arachnida (*E. californicum*) Hcs diverged about 450 millions of years ago. The X-ray crystallographic studies of deoxy-Hc from *Panulirus interruptus* [9] and the deoxy- and oxy-forms of *L. polyphemus* [8,10,11] have elicited a detailed picture of the active site. Crystal structure analysis shows that subunit II of *L. polyphemus* Hc consists of three domains.

The active site of *Limulus* Hc is deeply buried within the protein matrix, and a number of hydrophobic residues, including tryptophans, are involved in the active site pocket. The effects of denaturants such as guanidine hydrochloride (Gdn.HCl), pH, temperature, etc. have been studied by different methods [12–15]. In addition, the properties of arthropodan Hcs from *Callinectes sapidus* [16], *Homarus americanus* [17], *Palinurus vulgaris*, *Carcinus maenas* [18–20], *Maia squinado* [21] and those of the molluscan Hcs from *Rapana thomasiana* [22,23] and keyhole limpet [24] have been investigated under different experimental conditions in our laboratory.

The current investigations were undertaken to study the stability of two arthropodan Hcs, *L. polyphemus* and *P. vulgaris*, representatives for two orders, and to compare the data with other Hcs from the orders of Crustacea (Infraorders: Palinura, Astacidea and Brachyura) and Chelicerata (Infraorders: Xiphosura, Araneae and Buthidal) and to correlate them with X-ray data. We analyzed the stability of the quaternary structure and its influence on the stability of the different functional subunits, caused by guanidine hydrochloride and pH, using fluorescence spectroscopy.

2. Experimentals

2.1. Purification of the native proteins and their structural subunits

Hcs were prepared from the hemolymph of the crab *Carcinus aestuarii* [18], crab *M. squinado* [21], lobster *H. americanus* [17] and scorpion *Buthus sindicus* [25] by the methods as described in the given references and of the adult *L. polyphemus* and spiny lobster *P. vulgaris*. Before use, the *Limulus* and *Palinurus* Hcs, previously stored at −20 °C in the presence of 18% sucrose, was dialyzed at 4 °C against the 0.1 M sodium bicarbonate buffer, pH 9.5. The native Hc was dissociated by 24 h dialysis at the same buffer in the presence of 10 mM EDTA and 1 M urea. The protein was then loaded onto an ion exchange FPLC Resource 6 ml column (Pharmacia, Sweden), equilibrated with 0.1 M NaHCO3, pH 9.5, containing 10 mM EDTA and 1 M urea (Eluent A). Elution was performed with a non-linear NaCl gradient made by using a 1 M NaCl solution in the buffer mentioned above as eluent (Eluent B). The purity and molecular masses of structural subunits were determined by SDS-PAGE [26].

2.2. Enzymatic digestion

Three milligrams of one modified structural subunit C2 of *C. aestuarii* Hc was dissolved in 1 ml of 5 mM ammonium bicarbonate buffer, pH 8.2, and incubated with 50 μl trypsin solution (1 mg ml^{-1}) at room temperature for 15 h, followed by a further addition of 50 μl trypsin solution. Then, the reaction mixture (enzyme:protein ratio of 1:30 w/w) was incubated overnight at 37 °C. The generated peptides were separated by gel filtration on a Superdex 300 column (Pharmacia, Freiburg, Germany) at a flow rate of 2 ml min^{-1}, using water as eluent. The fractions were separated by reverse phase HPLC on a Nucleosil 100 RP-18 column (250 mm × 10 mm; 7 μm; Macherey-Nagel, Germany). The peptides were eluted (detection at λ = 214 nm) at a flow rate of 1 ml min^{-1} by applying the following gradient: 90% buffer A, 10% buffer B for 10 min, then 10–100% B in 70 min; A: 0.1% TFA in H_2O; B: 0.085%TFA, 80% acetonitrile and 20% H_2O. The collected fractions were further subjected to amino acid sequence analysis.

2.3. Amino acid sequences

Each subunit of *L. polyphemus* Hc was further purified on a HPLC Nucleosil RP C18 column using 0.1% TFA in H_2O as loading buffer and 0.085% TFA, 80% acetonitrile and 20% H_2O as eluting solution (eluent B). The following conditions were used: 10% B for 10 min; then, 10–100% B in 70 min at a flow rate of 1 ml min^{-1}. Peak fractions were dried and after dissolving in 40% methanol, 1% formic acid, they were subjected to automated Edman N-terminal sequencing (Procise 494A Pulsed Liquid Protein Sequencer, Applied Biosystems GmbH, Weiterstadt, Germany).

2.4. Preparation of apo-forms

Apo-Hcs were prepared after 48 h dialysis of the native protein against 50 mM Tris/HCl buffer containing 20 mM EDTA and 20 mM KCN, pH 8.0, at 4 °C, followed by dialysis against CN-free buffer.

2.5. UV spectroscopy

Hc concentrations of the proteins were determined spectrophotometrically (UVIKON spectrophotometer, model 930) at 278 nm using the following absorption coefficients (A_{280}): A = 1.35 ml (cm mg)$^{-1}$ for *M. squinado* [21], A = 1.17 ml (cm mg)$^{-1}$ for *L. polyphemus*, A = 1.34 ml (cm mg)$^{-1}$ for *H. americanus* [17] and A = 1.34 ml (cm mg)$^{-1}$ for *P. vulgaris*, all in 50 mM Tris/HCl buffer, pH 8.0. Molar concentrations were referred to 75 kDa as molecular mass for the species containing one bi-nuclear copper site [27]. The fraction of oxy-Hc was determined spectrophotometrically by measuring the absorbance ratio at 340 and 278 nm and assuming the values A_{340}/A_{278} = 0.21 for native fully oxygenated protein [27].

2.6. Fluorescence spectroscopy

Fluorescence emission spectra were recorded with a Perkin-Elmer Model LS5 spectrofluorimeter, equipped with a thermostatically controlled sample holder and a Model 3600 data station. Protein solutions had an absorbance at the excitation wavelength <0.05 to minimize the inner filter or self-absorption effects. Excitation at 295 nm was used for predominant measuring the fluorescence of tryptophyl residues. Spectra were corrected for background due to the solvent.

Fluorescence quantum yields were calculated using N-acetyl tryptophan amide (N-Ac-Trp.NH_2) with a quantum yield of 0.13 (λ_{ex}= 295 nm at 25 °C) as a standard [28]. The spectra of the protein and of the standard solutions were normalised for their absorbance at the excitation wavelengths.

Fluorescence lifetime measurements were carried out at 20 °C using a System PRA 2000 nanosecond single photon counting spectrofluorimeter and a nitrogen-filled flash lamp with full width at half-maximum (FWHM) of about 2.5 ns. The data were analyzed by convoluting the instrument response function $Y(t')$ with an assumed decay function $P(t)$, using the following relationship:

$$R_c(t) = \int Y(t')P(t-t')\,dt' \quad (1)$$

The $R_c(t)$ value obtained, was compared with the experimental time dependence $R_m(t)$. The accuracy in the excited state lifetime (τ) determination was 0.1 ns. The decay curves contained 10^4 counts at the maxima. The time interval for these curves was ±0.1 nsec per channel.

2.7. pH stability

Different species of Hcs were kept for 24 h in different buffers of the pH range 2–11.5 (0.05 M sodium citrate (pH 3.0–5.0); 0.05 M sodium phosphate (pH 5.0–7.0); 0.05 M Tris/HCl (pH 7.0–9.0); 0.05 M carbonate/bicarbonate pH (9.0–10.5) and 5 M NaOH (pH 11–12).

2.8. Denaturation in Gdn.HCl–water solutions

Fluorescence measurements were performed in 50 mM Tris/HCl buffer, pH 8.2, in the presence of 5 mM $CaCl_2$ and 5 mM $MgCl_2$ using a 10 mm quartz optical cell. The Gdn.HCl concentrations were stepwise (discrete) increased from 0 to 8 M denaturant. The tryptophan emission spectra were measured after equilibration for 24 h from 300 to 420 nm at an excitation wavelength of 295 nm.

3. Results and discussion

3.1. Purification of the native proteins and their structural subunits

The electron microscopic observations of native *M. squinado* [21], *H. americanus* [17], *B. sindicus* [25] Hcs reveal that these proteins exist as a mixture of four-, di- and mono-hexameric aggregates. The same results were observed for Hcs of *L. polyphemus* and *P. vulgaris*. The native molecule of *L. polyphemus* Hc was dissociated at 0.1 M $NaHCO_3$, pH 9.5, containing 10 mM EDTA and 1 M urea, then chromatographically separated on Resource column into five major fractions with molecular masses about 75 kDa (Fig. 1). In this case, the non-dissociated protein, eluting in the front of the chromatogram, accounts for 5% of total protein. Five fractions, indicated in Fig. 1 as L_1–L_5, can be separated as major components and are present >90% in the oxygenated form, as indicated by the A_{340}:A_{278} value 0.20.

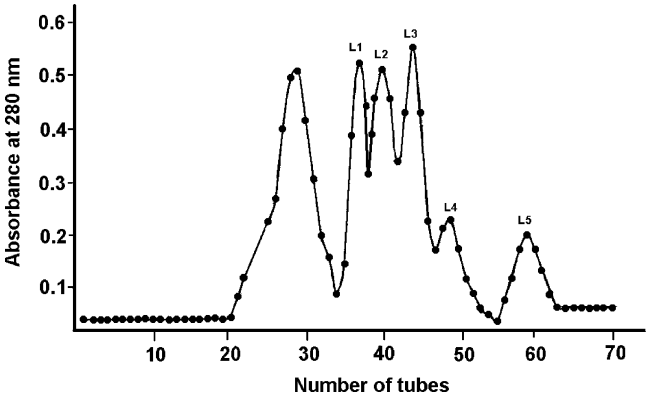

Fig. 1. Fast protein liquid chromatography (FPLC) of dissociated subunits on a Resource 6 ml column, equilibrated with 0.1 M $NaHCO_3$ buffer, containing 10 mM EDTA and 1 M urea, pH 9.5. Subunits were separated with a linear NaCl gradient (0–1 M) at a flow rate of 2.0 ml min^{-1}.

3.2. Active sit

The high overall sequence similarity between these proteins is particularly pronounced at their copper ions in the active sites A and B (CuA and CuB). The copper-binding sites of Crustacea *C. aestuarii* Hc were determined after digestion with trypsin followed by separation of the generated peptides via HPLC and sequenced. Two well-separated copper-binding regions – the CuA site close to the N-terminus and the CuB site near to the C-terminus have high sequence identity (Fig. 2A). According to the X-ray crystal structure, subunit II of the *Limulus* Hc is composed of three domains [7], and a bi-nuclear copper centre that reversibly binds oxygen is located in domain 2. Each copper ion is buried in the core of this domain and is coordinated by three histidine side chains (Fig. 2A). Alignment of partial sequences of CuA and CuB sites from structural subunit C2 from *C. aestuarii* and different structural subunits from other Crustacea (*Cancer magister* subunit Cm6, *P. interruptus* subunit Pic, *P. vulgaris* subunit Pv1) and second order Chelicerata (*Limulus polyphemus* subunit Lp1; *Euripelma californica* subunit Ece, *Androctonus australis* subunit Aa6) show considerable homology. Sixteen positions are conserved in the CuA site (Tyr162, Asn166, Gly168, Asp170, His172, His173, Trp176, His177, Pro181, Trp184, Asn194, Arg195, Lys196, Gly197, Glu198, His205, marked bold in Fig. 2B) with even higher homology, observed for the first three subunits Ca2, Cm6 and Pic and the last three subunits (Lp1, Ece and Aa6). In each subunit, the His residues in the copper-binding domain A, are conserved at positions 172, 173, 177 and 205 and at

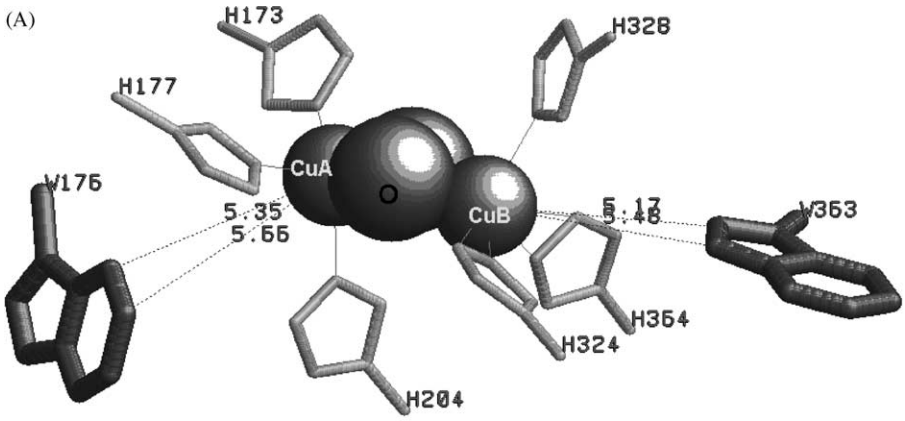

Distance between Trp residues and Cu ions in the active site of *L. polyphemus* Hc

	CuA	CuB	W65	W174	W176	W184	W326	W363	W538	W563
CuB (Å)	3.59	0.00	25.24	14.99	11.8.	18.89	13.36	5.17	16.16	30.88
CuA (Å)	0.00	3.59	22.80	12.02	5.36	17.09	15.82	9.08	13.88	28.54
Accessibility (%)			58.6	2.0	0.0	8.0	19.1	36.3	0.1	51.0

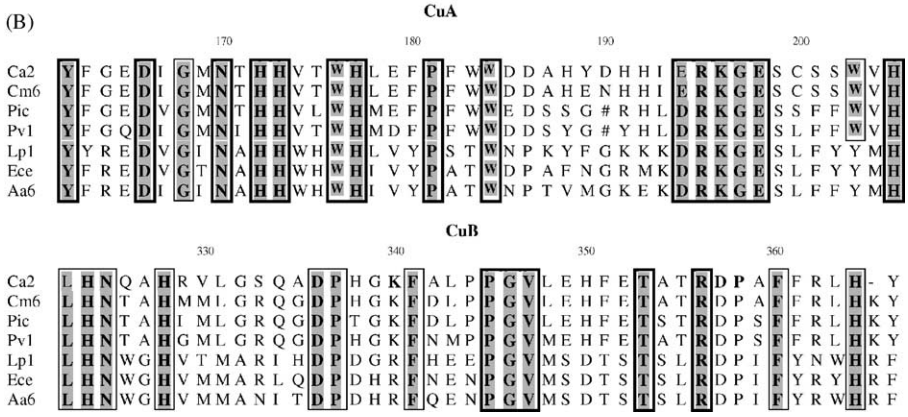

Fig. 2. (A) X-ray structure of active sites "A" and "B" of *Limulus polyphemus* Hc; (B) alignment of partial sequences around CuA and CuB sites from different structural subunits from the order of Crustacea: *Carcinus aestuarii* subunit Ca2, *Cancer magister* subunit Cm6 (GB AF091261), *Panulirus interruptus* subunit Pic (SP P80096), *Panulirus vulgaris* subunit Pv1 (SP P80888) and from second order of Chelicerata *L. polyphemus* subunit Lp1 (SP P04253), *Euripelma californica* subunit Ece (GB X16650) and *Androctonus australis* subunit Aa6 (SP P80476). SP: SwissProt accession no., GB: GenBank accession no.

positions 324, 328 and 364 in the copper-binding domain B. Seven or eight Trp residues are present in one structural subunit of arthropodan Hcs, where by three or four of them are located in CuA active site at positions 174, 176, 183, (184 or 203). One or two Trp residues are located near to the CuB site in Lp1, Ece, Aa6, while in Crustacea Hcs no Trp residue is found in the CuB site. Location of Trp residues in the active sites and near to the Cu-ions is influence fluorescence emission, which is statically quenched by Cu-ions.

3.3. Fluorescence properties

The fluorescence properties (quantum yield and λ_{max}) of these two orders of Crustacea and Chelicerata Hcs, are expected to be similar for both orders of Hcs, as a large numbers of tyrosine (about 720) and tryptophan residues (about 140) are found in the native molecule, corresponding to about 18 tyrosine and 7–8 tryptophan residues in one structural subunit. The emission spectra of *L. polyphemus* Hc from the order of Chelicerata are characterized by an emission band with a maximum at 333 ± 1 nm upon excitation at 295 nm, where the tryptophan residues are almost exclusively excited, which is in the same region as for other Hcs from this order (Table 1). *P. vulgaris* Hc has a λ_{max} of 326 ± 1 nm as other crustacean Hcs. The quantum yields for both are similar because they contain the same number of Trp residues. The shift of the emission maximum towards shorter wavelengths is diagnostic for tryptophyl side chains in a non-polar environment, since λ_{max} for Trp in water is 355–360 nm [28]. Comparison of the emissive properties of

Table 1
N-terminal sequences of different species of arthtropodan hemocyanins: Order Crustacia, Infraorders Palinura: *Palinurus vulgaris* (Pv); *Panulirus interruptus* (Pi) [31]; *Panulirus japonicus* (Pj) [32]; Astacidea: *Homarus americanus* (Ha) [22]; Brachyura: *Carcinus aestuarii* (Ca) [24]; *Maia squinado* (Ms) [25]; Order Chelicerate, Infraorders Xiphosura: *Limulus polyphemus* (Lp); Buthidae: *Buthus sindicus* (Bs) [26]; Araneae: *Euyrypelma californicum* (Ec) [33] and their fluorescence properties

Order: Crustacea																					λ_{max}		**Q**	
Infraorder Palinura																					oxy-	apo-	oxy-	apo-
	1				5					1 0				1 5					2 0					
Pv native																					326±1	335±1	0.012	0.082
Pva			D	V	H	S	S	D	N	**A**	H	**K**	**Q**	Q	D	V	**N**	H	L	L	D	K	333±1	338±1	0.024	0.096
Pvb			D	V	H	S	S	D	N	**A**	H	**K**	**Q**	H	D	V	**N**	H	L	L	D	K				
Pia			D	A	L	G	T	G	N	**A**	Q	**K**	**Q**	Q	D	I	**N**	H	L	L	D	K				
Pib			D	A	L	G	T	G	N	**A**	N	**K**	**Q**	Q	D	F	**N**	H	L	L	D	K				
Pic		G	D	S	A	D	K	L	L	**A**	Q	**K**	**Q**	H	D	V	**N**	Y	L	V	Y	K				
Pjla		G	D	S	T	D	K	L	L	**A**	Q	**K**	**Q**	D	D	V										
Infraorder Astacidea																								
Ha1					G	T	T	V	V	**A**	H	**K**	**Q**	Q	S	V	**N**	R	L	L	Y	K	336±1	338±1	0.053	0.120
Ha2					G		A	D	V	**A**	H	**K**	**Q**	Q	S	V	**N**	H	L	L	Y	L	335±1	337±1	0.058	0.110
Ha3		P	S	V	S	T	V	N	V	**A**	Q	**K**	**Q**	H	D	V	**N**	F	L	L	F	K	335±1	336±1	0.058	0.100
Ha4		G	A	Y	G		Q	G	Q	N	I	G	**Q**	L	F	V	**N**	I	L	I	F	L	334±1	338±1	0.056	0.110
Ha5			G	A	G	E	A	L	N	**A**	K	R	**Q**	Q	D	V	**N**	H	L	L	D	L	333±1	336±1	0.030	0.100
Ha6					S	P	A	F	Q	**A**	Q	**K**	**Q**	A	K	V	**N**	D	V	L	D	K	336±1	338±1	0.038	0.110
Infraorder Brachyura																								
Ca1	X	D	P	A	S	V	S	D	**A**	X	**K**	**Q**											336±1	336±1		0.106
Ca2						T	C	L	**A**	H	**K**	**Q**	Q	A	V	M	R	L	L	Y	R	335±1	338±1		0.093
Ca3		D	S	P	G	G	A	S	D	**A**	Q	**K**	**Q**	H	D	V	**N**	S	I	L	X	K	332±1	334±1		0.090
Ca4			D	Q	P	G	D	V	K	**T**	H	**K**	**Q**	**Y**	**D**	**V**	**N**	**Y**	**L**	**F**	**F**	**K**				
Ms1			D	Q	P	G	D	V	K	T	H	**K**	**Q**	Y	D	V	**N**	Y	L	F	F	K	336±1	337±1	0.028	0.082
Ms2							G	Q	L	**A**	L	**K**	**Q**	Q	T	V	**N**	R	L	L	N	K	333±1	337±1	0.030	0.080
Ms3							G	G	P	**A**	G	**K**	**Q**	N	A	V	**N**	Q	L	L	V	L	336±1	338±1	0.026	0.085
Ms4							D	G	P	**A**	Q	**K**	**Q**	N	T	V	**N**	Q	L	L	V	L	334±1	336±1	0.024	0.087
Ms5		D	H	A	G	T	V	S	K	**A**	H	**K**	**Q**	H	D	V	**N**	S	V	L	Y	K	333±1	335±1	0.025	0.085
Ms6					G	G	P	S	Q	K	Q	**K**	**Q**	H	K	V	**N**	L	V	N	I	K				
Order Chelicerate																								
Infraorder Xiphosura																								
L. native																					333±1	343±1	0.025	0.078
Lp1							**T**		L	H	**D**	**K**	**Q**	I	**R**	V	C	H	L	F	E	Q	340±1	347±1	0.043	0.109
Lp2							**T**		I	K	**E**	**K**	**Q**	K	**R**	X	N							346±1		0.098
Lp3								H	I	K	**E**	**K**	**X**	D	**R**	**I**	**L**							343±1		0.113
Lp4							**T**		I	K	**E**	**K**	**Q**	D	**R**	**I**	**L**							347±1		0.102
Lp5								X	L	Q	**E**	**L**	**Q**	A	H	**I**	**L**									
Infraorder Buthidal																								
Bs							**T**		V	L	**E**	K	**Q**	G	**R**	I	**L**	S	L	F			335±1	336±1	0.024	0.070
Infraorder Araneae																								
Eca					M		**T**	I	L	H	**D**	**K**	**Q**	V	Q	A	**L**	K	L	F	E	K	335±1	345±1	0.006	0.092
Ecb					M	P	**S**		T	A	**E**	**K**	**Q**	R	**R**	**I**	**L**	P	F	F	Q	F				
Ecc					M	P	**S**	D	A	N	**E**	M	**Q**	A	**R**	**L**	**L**	Q	L	F	E	H				
Ecd					M		**T**		I	A	**D**	H	**Q**	A	**R**	**I**	**L**	P	L	F	K	K				
Ece					M	P			D	K	Q	**K**	**Q**	L	**R**	V	**I**	S	L	F	E	H				
Ecf					M		**T**		V	Q	**D**	**K**	**Q**	R	Q	**I**	**L**	P	L	F	E	H				
Ecg					M	A	**S**		I	P	**E**	**K**	**Q**	A	L	**I**	**L**	P	L	F	E	K				

the oxy- and apo-forms under the same experimental conditions (50 mM Tris/HCl buffer, pH 8.2) shows that the quantum yield strongly increases for both, *Limulus* (Q_{oxy} = 0.025; Q_{apo-} = 0.078) and *P. vulgaris* (Q_{oxy} = 0.012; Q_{apo-} = 0.082) Hcs upon removal of copper from the active site. This effect is accompanied by a 10 nm shift of the emission maximum from 333 ± 1 nm (oxy-Hc) to 343 ± 1 nm (apo-Hc) (Table 1). Fig. 2A shows in detail the environment around the active site of *Limulus* Hc, where the positions of neighboured Trp residues are evidenced. Subunit II contains eight Trp residues: Trp65, Trp174, Trp176, Trp184, Trp326, Trp363, Trp538 and Trp563; however, not all of them are present in the various subunits of other hemocyanins. All Trp residues, with the exception of Trp563, are located in the second domain of *Limulus* Hc. Two of them (Trp176 and Trp363) are located within a small distance below 6 Å from CuA and/or CuB, respectively (Fig. 2A; Trp1765.36 Å from CuA site and Trp3635.17 from the CuB site). Trp174 (12.02 Å) and Trp538 (13.88 Å) are located also in the neighbourhood at the Cu site. The emission of these Trp residues in the oxy-form is strongly quenched by the Cu-ions. Removal of O_2 and copper ions drastically increases the tryptophan fluorescence (343 nm for the whole molecule and about 347 nm for the structural subunits). Fig. 2A shows that Trp176. . .CuA=O_2=CuB-His328 and Trp363. . .CuB=O_2=CuA-His177 are "parallel" to each of the "conjugated chains". The distance of Trp176. . .CuA (5.36 Å) is somewhat larger than Trp363. . .CuB (5.17 Å), but the first is "in touch" with the negative dipole side (CE3) of Cu(A) and the second Trp363 is "in touch" with Cu(B) with its positive dipole side (near CD1) and thus, both polarize CuA=O_2=CuB in a way that CuA could be more positively and CuB more negatively charged. The fluorescence of both Trp residues has to be strongly quenched by cupric ions in oxy-Hc and by their environment [29]. In the oxy-state, the distance between both Cu ions is 4.6 Å (CuA. . .4.6. . .CuB) and this is very understandable from an electrostatic point of view (repulsion). The Trp distribution around the active site is a strict peculiarity of *Eurypelma* Hc, actually, only 50% of the Trp residues in other Chelicerata Hcs are located near the copper ions and are distributed only in the vicinity of one metal center [3]. The access to Trp174, Trp176 and Trp538 for the quenchers is very low and different because their different static accessibility calculated as small as 2.0%, 0.0% and 0.1%, respectively.

These features of *Limulus* Hc explain the exceptionally strong quenching of the Trp fluorescence in the oxy-form, in comparison with other Hcs [21]. Fig. 2B shows that four Trp residues are located in the CuA site of Crustacea Hc and three in Chelicerata Hc, while only one or two Trp are present in the CuB site near to His residues. No Trp residue is observed in the CuB site in Crustacea Hc.

3.4. Fluorescence lifetime

Three classes of Trp-s are represented in native arthropodan Hcs. Some of them are located on the subunit surface, in the regions involved in inter-subunit contacts, as Trp563 in *Limulus* and Trp292 in *Euripelma* Hcs. The exposure of these residues to the solvent is connected with short-life time and they have calculated relative static accessibilities 58.6% and 36.3%, respectively. The distances between these two Trp residues and Cu-ions are four times higher than that between Cu and the Trp176 and Trp363 (Fig. 2A), and their emission cannot be quenched by internal Cu-ions. The emission of whole molecule is quenched by the microenvironment of the Trp residues and by the interaction of the subunits. Evidence for this is that the fluorescence quantum yield of whole molecule is less than that for its structural subunits (Table 1). The isolated subunits in the oxy-form as and their corresponding apo-forms exhibit quantum yields higher as compared to the whole Hc.

Moreover, the lifetime values of Hc remain almost constant upon O_2 and copper removal, changes being observed only in the normalized pre-exponentials A; this supports a mechanism of static quenching by copper ions of the active site [30]. Removing quenching Cu-ions from the active site of the molecule is connected with an increase of the quantum yield but not with τ_1. Thus, the increase of fluorescence quantum yield in apo-Hc must be attributed to the demasking of Trp fluorophores, which are fluorimetrically almost silent in the native protein. The fluorescence decay curve for Trp residues has been found to be multi-exponential in single as well as multiple Trp containing proteins. The multi-exponential decay arises due to the conformational isomers of the Trp residues, where the local environment of the indole chromophore differs substantially. The time-resolved fluorescence decay of *Limulus* Hc gave two lifetime components, which indicate possible presence of two alternative Trp-positions ("conformational alternates") (Fig. 3). The fluorescence decays of the parent molecule, the two subunits, and N-Ac-Trp.NH_2, excited at 295 nm, well fitted to two exponentials. The theoretical fluorescence intensity is given by the function

$$P(t) = A_1 e^{-t/\tau_1} + A_2 e^{-t/\tau_2} \quad (2)$$

where A_1 and A_2 are amplitudes. This function was used for the determination of the excited state lifetimes. Analysis of the data in terms of bi-exponential models give a good fit between the experimental and theoretical curves. The values show that the environment of these chromophores significantly influences their dynamic fluorescence characteristics. The lifetimes for the native molecule of arthropodan *L. polyphemus* Hc are very short (τ_1 = 0.3 ns, τ_2 = 3.3 ns), but higher than for molluscan keyhole limpet Hc (τ_1 = 0.2 ns, τ_2 = 2.6 ns) [24]. Our experimental data as well as the data from similar structures gives us the reason to suggest that Trp563 and Trp65 seems to be short-lived (τ_1 = 0.3 ns) and their emission (81%) is almost completely quenched and Trp197 and Trp346 are long-lived (τ_1 = 2.56 ns) with emission of about 18%. The fluorescence decay properties clearly differ between the whole molecule and the subunits, which suggests

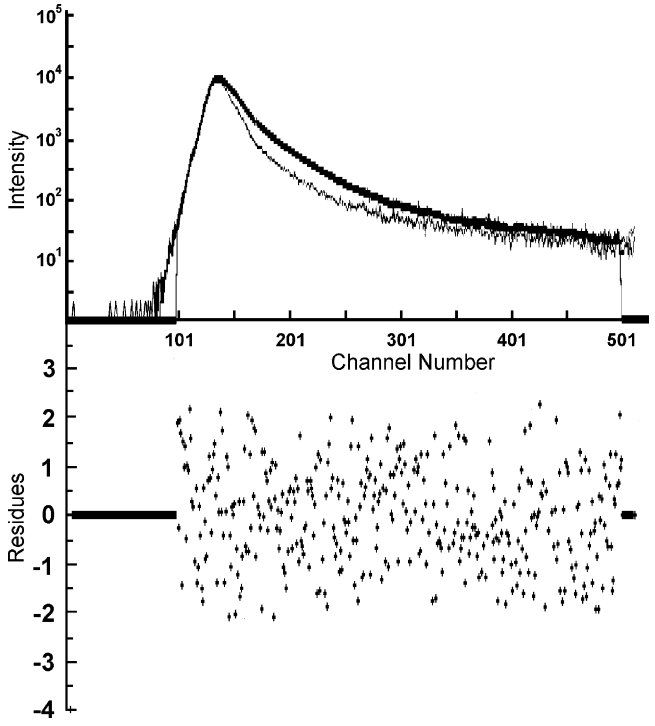

Fig. 3. Fluorescence decay of whole *L. polyphemus* Hc molecule in 0.05 M Tris/HCl, buffer with 5 mM $CaCl_2$ and $MgCl_2$, pH 8.2 after excitation at 295 nm.

that the respective tryptophans are affected differently by the local tertiary structure. The specific environment of the indole groups in *Limulus* Hc decreases the excited state lifetime by a factor of two in comparison with the value, determined for its subunits.

3.5. Denaturation with Gdn.HCl

The unfolding of proteins in denaturing compounds has been widely investigated. In the case of oligomeric proteins, inactivation, dissociation and unfolding have been described as the structural events that occur subsequently during the denaturation process. The present paper reports the changes in conformation and aggregation of tetrameric Hcs during unfolding in guanidine hydrochloride. The denaturation of these proteins takes place in several stages. Fig. 4A shows the fluorescence spectra of the whole molecule of *L. polyphemus* Hc at different concentrations of Gdn.HCl. The addition of denaturant concentrations between 0 and 1.5 M produced a slight increase of the fluorescence intensity, but at 2 M Gdn.HCl, the emission is higher and the quenching of Cu-ions is eliminated. At 2.0 M guanidine buffer, the whole molecule is fully dissociated into its structural subunits. The results are consistent with an aggregation occurring at 0.5 M guanidine, followed by a similarly drastic dissociation to give a monomeric protein unfolding at 1.5–2 M guanidine. Further increase of denaturant concentration decreases the intensity and is connected with a shift of λ_{max} towards 355 nm (red shift) as shown in Fig. 4A, which can be explained, by protein unfolding and guanidinium ion quenching.

The curves in Fig. 4B insert, expressing the unfolding of oxy-Hc at different concentrations of Gdn.HCl is analogous to the curve in Fig. 4C (expressing the unfolding of apo-Hc), but with specific changes in quaternary structure fluorescent properties (Fig. 4B insert, limb-a), which seems to represent two transitions. The first transition has a similar "position" (C_m = 0.52) and amplitude (dQ) typical for very quenched total Trp fluorescence. Obviously, this observation is due to quencher, the effect of which is removed at the followed unfolding step at C_m^* = 1.77 and with very big amplitude and sharpness of the transition (within 1.6 M interval). The only explanation is that in this step the Cu=O_2=Cu. . .Trp(s) native structure is destroyed causing a rise of Trp fluorescence. After this apparent "peak" of the amplitude (Q) and C_m in the curve for oxy-Hc, the following limb-b has analogous (but not the same) behaviour as in the apo-Hc case. Three unfolding steps with apparent C_m^* at 2.56, 4.41 and 6.77 M, respectively, could be identified in Fig. 4B insert, limb-b. The first of them (at the same amplitude) with ΔC_m = 1.2 is much sharper not only than the other two steps, but also in comparison with the first transition step with ΔC_m = 3.5 in case of the apo-Hc (Fig. 4C). The C_m^* of the next two transitions are at slightly lower Gdn.HCl concentrations, but with analogous small cooperatively. This behaviour can be explained assuming non-symmetric interactions between structural domains in the holo-protein, i.e. at the Cu=O_2=Cu site, formation of intra-subunit and chain–chain interactions are changed and the active site formation is coupled with structural alterations. Because the first (less-stable) domain is Cu site-dependent it can be selected from the known 3D-structure and the rest of two domains should be easily assigned in terms of their stabilities.

For a better understanding of the unfolding process of oxy-Hc, we have compared the Q(C_m) curve (Fig. 4B insert) with the R_{eff}(C_m) curve shown in Fig. 4B. The "velocity" of R_{eff} changes is different for the first two processes, showing their different nature (mark in the figure as regions I and II). Notably, the first domain (at the active site) transition fall in the same region II as previous ones and all of them are definitely cooperative. The other two transitions are without drastic changes of Trp environment after the unfolding.

Fig. 4C shows the fluorescence intensity of apo-Hc at different concentrations of guanidine hydrochloride. Quenching by Cu-ions is eliminated and the Q at 0 M Gdn.HCl is higher than for the oxy-form, but less than for structural subunits. In case of whole multi-chain apo-Hc, ("all apo-Hc"), the unfolding curve is more complex, but logically altered. It contains two limbs: (a) at low Gdn.HCl concentrations (0.0–2.4 M) and (b) at higher concentrations of denaturant (2.5–8.0 M). The last (b) limb-b exhibits also a three-step process as described above, but only the effective C_m^* values for oxy-Hc (Fig. 4B insert) are 0.6–0.7 higher than those for the apo-Hc (Fig. 4C). This means, the formation of the quaternary structure increases the stability in each of the three domains

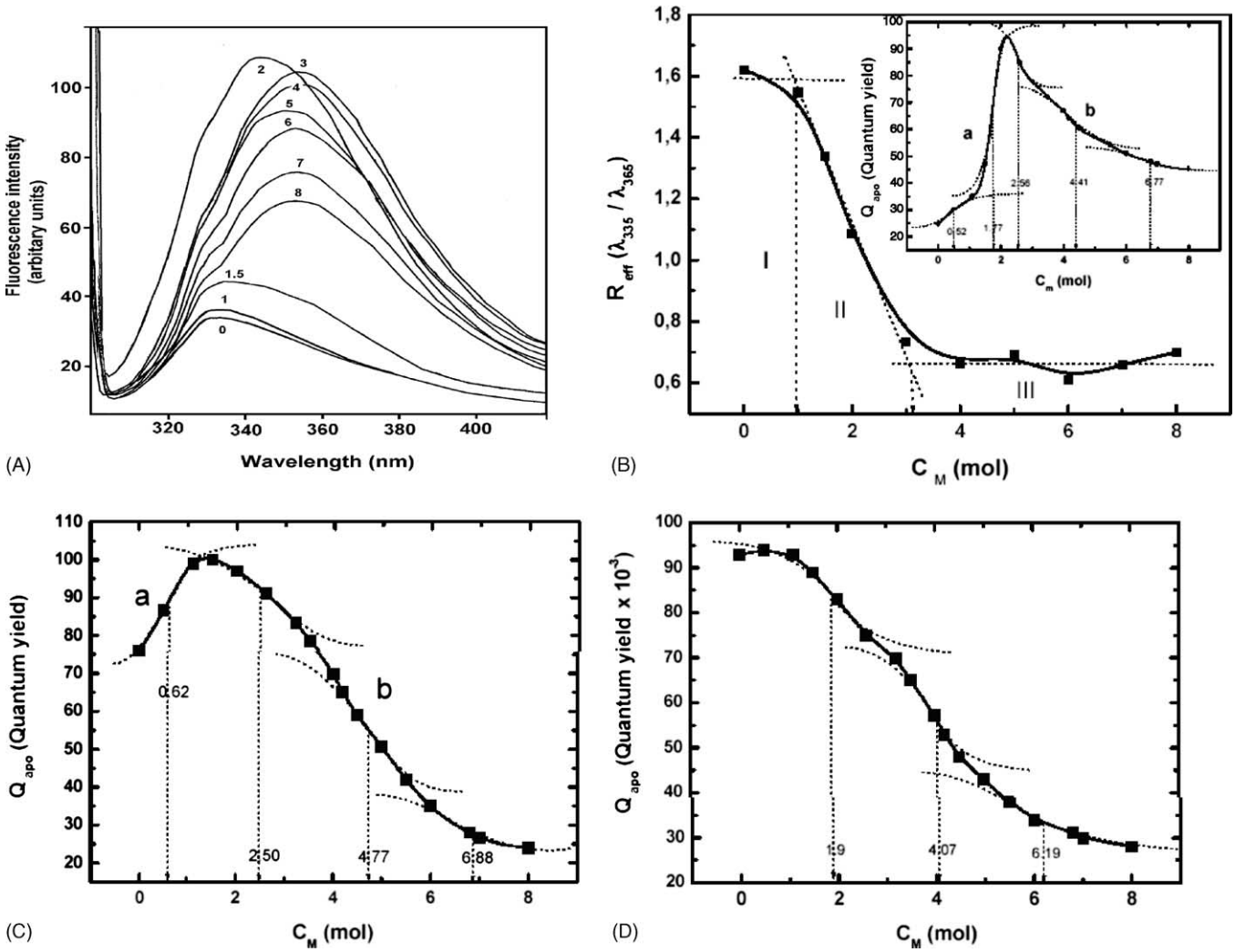

Fig. 4. (A) Emission spectra of oxy-whole molecule of *L. polyphemus* Hc at different concentrations (0–8 M) of Gdn.HCl. (B) R_{eff} at different concentrations of Gdn.HCl; (b-insert). Effect of guanidine hydrochloride on the stability of *L. polyphemus* native oxy-Hc molecule. (C) Effect of guanidine hydrochloride on the stability of *L. polyphemus* apo-Hc molecule. (D) Effect of guanidine hydrochloride on the stability of *L. polyphemus* oxy-subunit. The protein concentrations are about 0.05 mg ml^{-1} in 0.05 M Tris/HCl buffer with 5 mM $CaCl_2$ and $MgCl_2$, pH 8.2. The fluorescence quantum yield was determined using N-Ac-Trp.NH_2 as a standard.

and this alteration is approximately equal and independent for each of the domains. The presence of limb-a confirms the presence of a quaternary structure that is most sensible and easily destroyed at very low denaturant concentrations. From these results follows that multi-chain complex decomposition leads to an increase of apparent Trp fluorescence and we have to conclude that chain-chain interactions function as a moderate quencher of Trp fluorescence. This can be done by introduction of quenching groups to the given Trp residue(s) and/or by structural changes in the vicinity of the Trp residue(s) after polypeptide complex formation.

In Fig. 4D, the influence on one structural subunit "a" is shown expressing the conformational stability only for this protein. The single polypeptide Hc subunit undergoes unfolding in water–Gdn.HCl solutions as a multi-step process. Because the interval of the Q-change is very wide (from 1 to 8 M Gdn.HCl) and using the present shape the curve was deconvoluted into three sigmoid curves with apparent midpoints (C_m^*) at 1.90, 4.07 and 6.19 M, respectively. It is known from 3D X-ray analysis [7] that this subunit contains three structural domains and we can speculate to assign each of the processes to each of these domains. This hypothesis requires domains to differ considerable in stability at a ratio of approximately 1:2:3. We hope to prove this suggestion from specially designed experiments, now in progress. On the basis of the above discussion, a model is given summarizing the results is as follows:

$$\mathrm{Tn} \Leftrightarrow \mathrm{Tn}' \Leftrightarrow \mathrm{A} \Leftrightarrow \mathrm{Mn}' \Leftrightarrow \mathrm{Mu} \quad (3)$$

In this model, Tn represents native tetrameric protein that, at low guanidine concentrations, forms an active intermediate (Tn′) with more hydrophobic surfaces exposed to the solvent. As the guanidine hydrochloride concentration increases, further exposure of hydrophobic interaction area lead to the

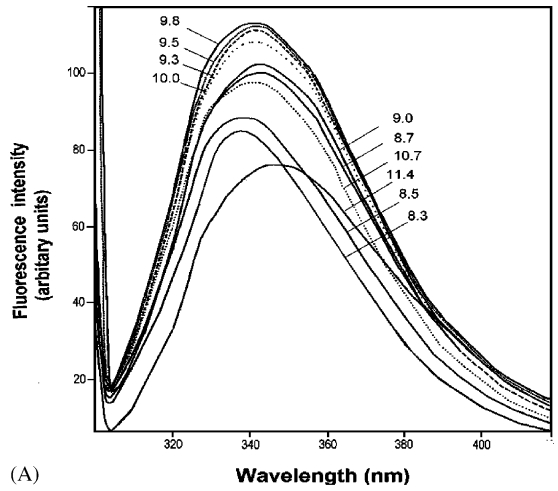

(A)

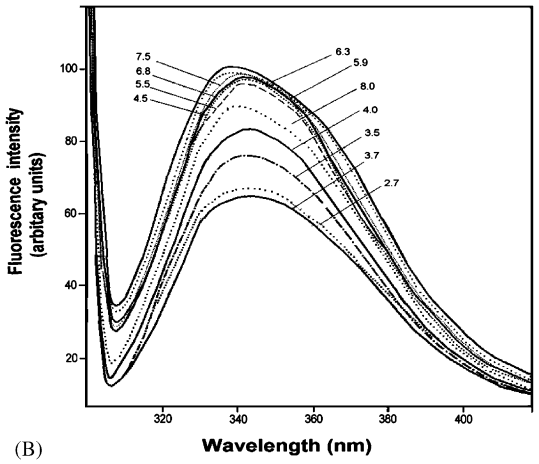

(B)

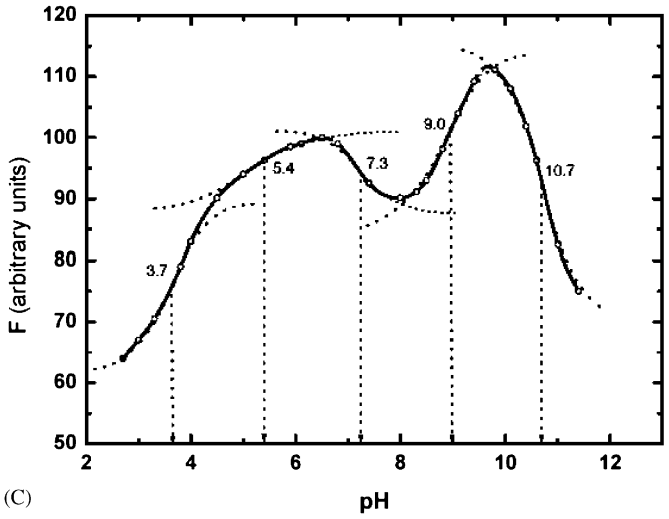

(C)

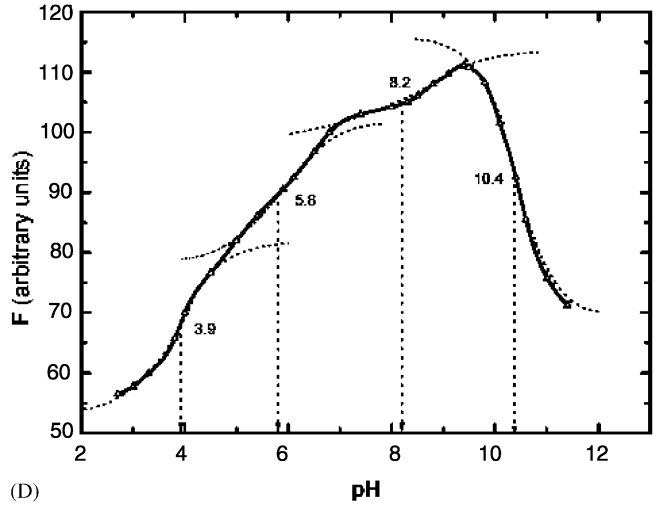

(D)

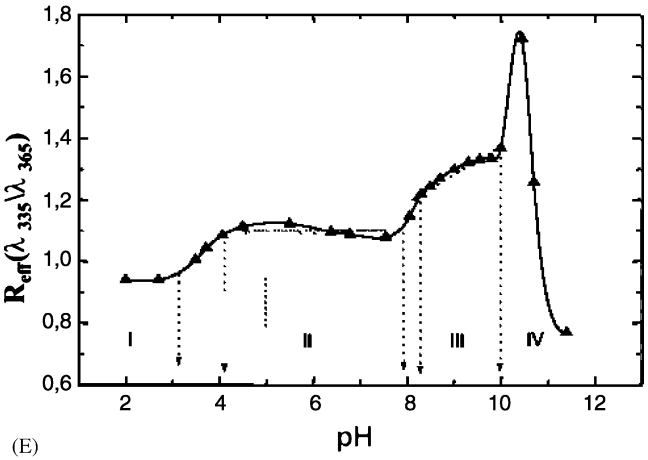

(E)

Fig. 5. (A) Emission spectra of native *L. polyphemus* oxy-Hc in the pH region (9–11.5) and (B) in pH region (2–8.5). (C) Effect of pH on the stability of native *L. polyphemus* oxy-Hc. (D) Effect of pH on the stability of *L. polyphemus* apo-whole molecule. (E) R_{eff} at different pH. The protein concentrations are about 0.05 mg ml^{-1} in 0.05 M Tris/HCl buffer with 5 mM $CaCl_2$ and $MgCl_2$, pH 8.2. The fluorescence quantum yield was determined using N-Ac-Trp.NH_2 as a standard.

formation of aggregated species (A). Finally, at concentrations higher than 2.0 M guanidine-HCl, the highly aggregated species dissociate into partly unfolded monomers (Mn′) that are eventually completely unfolded (Mu), accompanied by a further increasing maximum fluorescence emission.

3.6. Effect of pH on the stability

Finally, we also measured the effect of pH in the range from 2.0 to 12.0 on the tryptophan fluorescence of *L. polyphemus* Hc and one structural subunit. Fig. 5A and B shows the fluorescence spectra on *L. polyphemus* oxy-Hc recorded at different values pH intervals (8–11.4 and 8–2.5). The pH-dependence of Trp-fluorescence quantum yield (Q) of native oxy-Hc is shown in Fig. 5C. In the acidic pH-region (3.5–6.5), two proton bindings, influencing the quantum yield, were observed with crude resolved p*K*s at 3.7 and 5.4. The first is tentatively addressed to Asp (p*K* = 3.7) or Glu ionization(s) and exhibits cooperative behaviour (it involves more than one proton uptake within the pH interval, i.e. the sharpness of Q(pH)-transition is larger than one). Based on cooperative behaviour, this transition can be also an acid denaturation one and its nature will be proven later based on CD measurements. The second acidic pH-dependent Q-change is three times smaller in amplitude, with a crude effective p*K* = 5.4 and not cooperative. Again, this may be a single carboxyl group ionization being in a negative electrostatic potential field. However, and more probably, it is due to a single His ionization located close to positively charged $Cu^{(2+)}$ ion and near to Trp, the deprotonation of which partially removes its quenching effect. Most interesting is the Q(pH) behaviour at the neutral pH region (6.5–9.5) with two contrary processes: deprotonation of first site(s) increase Trp quenching (diminish *Q*) with a crude p*K* of 7.3 and obvious cooperativity and of second one with a crude p*K* of 9.0, causing decoupling of Trp fluorescence quenching. Probable candidates for both sites should be His residues in the Cu^{2+} vicinity or coupled ionisation of α-amino groups at the N-terminus.

Since the equilibrium constant of Hc for oxygen binding is expected to change as a function of pH, the experiments have been carried out on the Apo-proteins (Fig. 5D) in order to avoid the complications due to the change in fluorescence intensity depending on the shift in the position of the oxygen-binding equilibrium and compared with pH denaturation of oxy-Hc. Disappearance of the first transition (p*K* = 7.3) in apo-Hc leads to the conclusion for O_2-binding-dependent ionization (in analogy to well known for hemoglobins Bohr-effect). The last "alkaline ionization" at p*K* = 10.7 is obviously connected with the loss of the Cu^{2+} ion(s) and followed by alkaline denaturation. Removal of the oxygen from Cu^{2+}-binding centre of Hc leads to the characteristic change to its pH-dependent intrinsic (Trp-s) fluorescence. The *Q*(pH) shape is different in the pH region of 6.5–9.5 in comparison to that for oxy-Hc (Fig. 5C). Both "processes", observed for oxy-Hc (with pK_{app} 7.3 and 9.0, respectively) are substituted by a one "process" in apo-Hc with positive tangent and apparent pK_{app} = 8.2, leading to Trp-fluorescence increasing. This single process can be addressed to the "second" one in the oxy-Hc, but with pK shifted from 9.0 to 8.2 ($\Delta pK = 0.8$). The effect could be complex: omitting O_2 (a bi-radical particle, Trp fluorescence quencher) should increase both, the Trp quantum yield and the "amplitude" of the *Q*(pH) transition with an effective p*K* = 5.8, which is shifted by 0.4 pH units compared to a p*K* = 5.4 in oxy-Hc. This is connected to small conformational changes of His and Trp residues in the O_2-binding site. Two types of Trp–His couplings by non-contact coplanar π–π interactions were identified. One is located within the Cu center (W176...H173 and W363. . .H324) and the second one through Cu–O_2–Cu bridge (W176. . .H328 and W363. . .H177). Removal of O_2 in deoxy-Hc will change the distances between Trp and His and Trp. . .Cu(O_2), and especially their orientations. Both transitions in oxy-Hc (with p*K* 7.3 and 9.0, respectively) are cooperative (see above), while the single transition in apo-Hc (with p*K* 8.2) is a non-cooperative one and is addressed to single group ionization. Both, the acidic and alkaline limbs (p*K* 3.9 and 10.4, respectively) in Fig. 5D are slightly drawn together. The calculated values from the curves in Fig. 5C and D for the oxy- and apo-Hcs ($dpK = pK_{al} - pK_{ac}$) are 7.0 and 6.5, respectively, i.e. they differ in 0.5 pH units, which qualitatively in agreement that O_2-binding to the active site stabilizes the Hc structure.

The spectral position of the apparent Trp fluorescence band which is a sum of individual contributions of each emitted single Trp residues, is also pH sensitive and defines their summary position and shape by the ratio of fluorescent intensities (R_{eff}) at two arbitrary wavelengths (335 and 365 nm were selected):

$$R_{eff} = \frac{I_{\lambda(335)}}{I_{\lambda(365)}} = f(\mathrm{pH}) \quad (4)$$

Both limbs with p*K*s 3.7 and 10.7 shown in Fig. 5E overlap the regions of changeable pH/R_{eff} values, i.e. the structure are "in transition". The same could be said for the transition with p*K* = 9.0, but at this pH the protein is native what allows to speculate that this transition is coupled with change in Trp orientation(s). It seems that the both others transitions with p*K* values of 5.4 and 7.0, respectively, proceed without structural changes altering Trp micro-environment(s).

Acknowledgments

P. D-A. would like to thank Deutsche Forschungsgemeinschaft (DFG) and Deutscher Akademischer Austausch Dienst (DAAD) for granting a scholarship. This work was supported by grants from DLR 01/001 and from the NCSI (X-1302) of the Ministry of Education and Science, Bulgaria. One of the authors (PN) is deeply grateful to the Swedish Council for Planning and Coordination of Research (Grant N a 1-5/2286) for the financial support, which allowed performing the fluorescence lifetime measurements.

References

[1] K.E. van Holde, K.I. Miller, Adv. Protein Chem. 47 (1995) 1.
[2] B. Salvato, M. Beltramini, Chem. Rep. 8 (1990) 1.
[3] E. Hodgson, J.I. Spicer, Comp. Biochem. Physiol. Part A 128 (2000) 873.
[4] K.E. Van Holde, K.I. Miller, H.J. Decker, Biol. Chem. 19 (2001) 15563.
[5] D. Sancher, M.D. Gantornin, G. Gutierrer, M.J. Bastiani, Mol. Biol. Evol. 15 (1998) 415.
[6] R. Topham, S. Tesh, G. Cole, D. Mercatante, A. Westcott, C. Bonaventura, Arch. Biochem. Biophys. 352 (1998) 103.
[7] K.A. Magnus, B. Hazes, H. Ton-That, C. Bonaventura, J. Bonaventura, W.G.J. Hol, Proteins Struct Funct Genet 19 (1994) 302.
[8] A.K. Shrive, A.M. Metcalf, J.R. Cartwright, T.J. Greenhough, J. Mol. Biol. 290 (1999) 997.
[9] A. Volbeda, W.G.J. Hol, J. Mol. Biol. 209 (1989) 249.
[10] B. Hazes, K.A. Magnus, C. Bonaventura, J. Bonaventura, Z. Dauter, K.H. Kalk, W.G.J. Hol, Protein Sci. 2 (1993) 597.
[11] K.A. Magnus, H. Ton-That, J.E. Carpenter, Chem. Rev. 94 (1994) 727.
[12] M. Guzman-Casado, A. Parody-Morreale, P.L. Mateo, J.M. Sanchez-Ruiz, Eur. J. Biochem. 188 (1990) 181.
[13] R. Sterner, T. Vogl, H.-J. Hinz, F. Penz, R. Hoff, R. Föll, H. Decker, FEBS Lett. 364 (1995) 9.
[14] R. Hübler, B. Fertl, N. Hellmann, H. Decker, Biochim. Biophys. Acta 1383 (1998) 327.
[15] M.A. Menze, N. Hellmann, H. Decker, K. Grieshaber, Biochemistry 39 (2000) 10806.
[16] S. Stoeva, P. Dolashka, B. Bankov, W. Voelter, B. Salvato, N. Genov, Spectrochim. Acta Part A 51 (1995) 1965.
[17] P. Dolashka-Angelova, S. Stoeva, R. Hristova, J. Schuetz, M. Beltramini, B. Salvato, W. Voelter, Curr Top. Pept. Protein Res. 3 (1999) 19.
[18] R. Hristova, P. Dolashka, S. Stoeva, W. Voelter, B. Salvato, N. Genov, Spectrochim. Acta Part A 53 (1997) 471.
[19] P. Dolashka-Angelova, R. Hristova, S. Stoeva, W. Voelter, Spectrochim. Acta Part A 55 (1999) 2927.
[20] P. Dolashka-Angelova, M. Beltramini, A. Dolashki, B. Salvato, R. Hristova, W. Voelter, Arch. Biochem. Biophys. 389 (2001) 153.
[21] P. Dolashka-Angelova, S. Stoeva, R. Hristova, J. Schuetz, W. Voelter, Spectrochim. Acta A 56 (2000) 1985.
[22] P. Dolashka, N. Genov, K. Parvanova, W. Voelter, M. Geiger, S. Stoeva, Biochem. J. 315 (1996) 139.
[23] P. Dolashka-Angelova, M. Schick, S. Stoeva, W. Voelter, J. Biochem. Cell Biol. 32 (2000) 529.
[24] J. Schütz, P. Dolashka-Angelova, R. Abrashev, P. Nicolov, S. Stoeva, W. Voelter, Biocim. Biophys. Acta 1546 (2001) 325.
[25] S.A. Ali, A. Abbasi, S. Stoeva, R. Kayed, P. Dolashka-Angelova, H. Schwarz, W. Voelter, Comp. Biochim. Physiol. Part B 126 (2000) 361.
[26] U.K. Laemmli, Nature 227 (1970) 680.
[27] L. Bubacco, R.S. Magliozzo, M. Beltramini, B. Salvato, J. Peisach, Biochemistry 31 (1992) 9294.
[28] M. Tabak, G. Sartor, P. Neyroz, A. Spisni, P. Cavatorta, J. Luminesc. 46 (1990) 291.
[29] N.B. Terwilliger, L. Dangott, M. Ryan, Proc. Natl. Acad. Sci. U.S.A. 96 (1999) 2013.
[30] T. Burmester, Mol. Biol. Evol. 18 (2001) 184.
[31] B. Neuteboom, P.A. Jekel, J.J. Beintema, Eur. J. Biochem. 206 (15) (1992) 243.
[32] N. Makino, S. Kimura, Eur. J. Biochem. 173 (2) (1988) 423.
[33] R. Voit, G. Feldmaier-Fuchs, T. Schweikardt, H. Decker, T. Burmester, J. Biol. Chem. 15 (275) (2000) 39339.